



Published in final edited form as:

*J Phys Chem B*. 2008 September 18; 112(37): 11770–11776. doi:10.1021/jp802629e.

## Raman Spectroscopy Reveals Direct Chromophore Interactions in the Leu/Gln105 Spectral Tuning Switch of Proteorhodopsins

Joel M. Kralj<sup>†</sup>, Elena N. Spudich<sup>‡</sup>, John L. Spudich<sup>‡</sup>, and Kenneth J. Rothschild<sup>\*†</sup>

<sup>†</sup>Department of Physics, Molecular Biophysics Laboratory, Photonics Center, Boston University, 590 Commonwealth Avenue, Boston, Massachusetts 02215

<sup>‡</sup>Center for Membrane Biology, Department of Biochemistry and Molecular Biology, University of Texas Medical School, Houston, Texas 77030

### Abstract

Proteorhodopsins are an extensive family of photoactive membrane proteins found in proteobacteria distributed throughout the world's oceans which are often classified as green- or blue-absorbing (GPR and BPR, respectively) on the basis of their visible absorption maxima. GPR and BPR have significantly different properties including photocycle lifetimes and wavelength dependence on pH. Previous studies revealed that these different properties are correlated with a single residue, Leu105 in GPR and Gln105 in BPR, although the molecular basis for the different properties of GPR and BPR has not yet been elucidated. We have studied the unexcited states of GPR and BPR using resonance Raman spectroscopy which enhances almost exclusively chromophore vibrations. We find that both spectra are remarkably similar, indicating that the retinylidene structure of GPR and BPR are almost identical. However, the frequency of a band assigned to the retinal C13-methyl-rock vibration is shifted from 1006 cm<sup>-1</sup> in GPR to 1012 cm<sup>-1</sup> in BPR. A similar shift is observed in the GPR mutant L105Q indicating Leu and Gln residues interact differently with the retinal C13-methyl group. The environment of the Schiff base of GPR and BPR differ as indicated by differences in the H/D induced down-shift of the Schiff base vibration. Residues located in transmembrane helices (D–G) do not contribute to the observed differences in the protein–chromophore interaction between BPR and GPR based on the Raman spectra of chimeras. These results support a model whereby the substitution of the hydrophilic Gln105 in BPR with the smaller hydrophobic Leu105 in GPR directly alters the environment of both the retinal C13 group and the Schiff base.

### 1. Introduction

Proteorhodopsins are a recently discovered class of photoactive proteins found primarily in proteobacteria which reside in all the world's oceans.<sup>1–5</sup> Harvesting sunlight, they use the absorbed energy to pump protons across the cell membrane or transduce a photon signal.<sup>1,6</sup> Due to their ubiquity, proteorhodopsins are thought to play a major role in solar energy transduction in the biosphere.<sup>2</sup> Since the initial discovery in Monterey Bay, shotgun genetic techniques have identified over 4000 variants spread across every ocean and also in freshwater.<sup>3–5,7</sup> Most variants can be divided into two main classes depending on their properties: green-absorbing proteorhodopsin (GPRs),<sup>1,8,9</sup> and blue-absorbing proteorhodopsin (BPRs).<sup>2,10</sup>

GPR, the earliest discovered proteorhodopsin in SAR-86  $\gamma$ -proteobacteria, has been the most extensively studied. GPR exists in shallow ocean depths, pumps protons with a fast photocycle (~20 ms) and has been shown to provide power for the cell under anaerobic conditions.<sup>11</sup> BPR which is typically found near the edge of the photic zone (75 m) and in the open ocean away from the shore,<sup>5</sup> has a blue-shifted visible absorption near 490 nm and slower photocycle (~200 ms) relative to GPR. These differences have been attributed to natural Darwinian selection given the lower intensity and blue shift of available sunlight at 75 m below the surface.<sup>2-12</sup>

It has been found that the substitution of only one residue in GPR (L105Q) switches the visible absorption and photocycle kinetics to the BPR phenotype.<sup>10,13</sup> Likewise the reverse mutation in BPR (Q105L) produces a red-shifted absorption maximum similar to GPR, but does not accelerate the photocycle.

In order to better understand the molecular basis for the above effects, we used resonance Raman spectroscopy (RRS) to compare chromophore structure and protein–chromophore interactions of GPR and BPR. RRS has been used previously to study other rhodopsins including mammalian visual rhodopsin,<sup>14</sup> bacteriorhodopsin,<sup>15-20</sup> sensory rhodopsin I and II,<sup>21-23</sup> halorhodopsin,<sup>24</sup> and Anabaena sensory rhodopsin.<sup>25,26</sup> Due to resonant enhancement of vibrations of the retinal chromophore when the excitation wavelength is near its visible absorption wavelength, retinal bands dominate the Raman spectra of rhodopsins, even when the excitation wavelength is far from the chromophore absorption maximum wavelength, such as in the case of BR. With a 1060 nm excitation and 570 nm visible absorption maximum, preresonance conditions still lead to significant enhancement of vibrational bands of the chromophore relative to protein bands.<sup>27</sup> Thus, the use of near-IR 785 nm excitation allows us to probe the vibrational spectrum of the retinal chromophore without significant interference from protein bands or photocycle intermediates that appear due to driving the photocycle with visible light.

In this study, Raman spectroscopy with 785 nm excitation was used to investigate the chromophore structure and protein–chromophore interaction of residue 105 in GPR and BPR. It is found that the chromophore structures of both variants of proteorhodopsin are remarkably similar. However, differences are detected which are attributable to changes in the interaction of residue 105 near the C13-methyl and Schiff base groups of retinal which may account for most of the differences in the properties of BPR and GPR.

## 2. Methods and Materials

### Protein Expression and Purification

*Escherichia coli* cells containing the GPR (Monterey Bay strain EBAC 31A8) or BPR (Hawaii Ocean Time strain HOT75M4) were cultured on standard Luria Broth Media (Sigma Aldrich) and supplied with either all-*trans* retinal or all-*trans* retinal containing a deuterium on carbon 15 ( $15C-^2H$ ). All procedures for the site-directed mutagenesis, plasmid construction and expression in the *E. coli* UT5600 strain were identical to those described previously.<sup>8</sup> Two chimeric constructs were made by PCR using the megaprimer method: B3G4 encodes the N-terminal portion of BPR up to Leu128 followed by the C-terminal portion of GPR. Conversely, G3B4 encodes the N-terminal portion of GPR up to Leu128 followed by the C-terminal portion of BPR. The nomenclature indicates the numbers of transmembrane helices from BPR and GPR that comprise the proteins encoded.

After the induction period, the cells expressing His-tagged wild-type or mutant PRs were centrifuged at 1000g, resuspended in 5 mM MgCl<sub>2</sub>, 150 mM Tris-HCl, pH 7.0, and disrupted by sonication. Unbroken cells were removed by low speed centrifugation. The

membranes containing pigment were collected by centrifugation (39000*g*, 30 min) and solubilized in a wash buffer (50 mM KPi, 300 mM NaCl, 5 mM imidazole and 1.5% octylglucoside (OG), pH 7.0) for at least 1 h at 4 °C. Unsolubilized membranes were removed by centrifugation at 28,000*g* for 30 min. The supernatant was incubated with a Hisbinding resin on a shaker at 4 °C for at least 1 h. The bound resin was applied to a 10 cm chromatography column and washed with 3× volume of wash buffer followed by elution buffer (50 mM KPi, 300 mM NaCl, 250 mM imidazole and 1.0% OG, pH 7.0). The sample purity was assessed by the UV–visible spectroscopy and SDS-PAGE analysis.<sup>1</sup>

### Proteoliposome Reconstitution

Purified His-tagged PR was reconstituted in *E. coli* polar lipids (Avanti, Alabaster AL) at a 1:10 protein-to-lipid (w/w) ratio. Lipids initially dissolved in chloroform were dried under argon and resuspended in the dialysis buffer (50 mM K phosphate, 300 mM NaCl, pH 7.0) to which OG was added to a final concentration of 1%. The lipid solution was incubated with the OG-solubilized protein for 1 h on ice and dialyzed against the dialysis buffer with 3 buffer changes every 24 h. The reconstituted proteoliposomes were pelleted by centrifugation and resuspended in the sample buffer (50 mM CHES, 150 mM NaCl, pH 9.5).

### Resonance Raman Spectroscopy

Approximately 50  $\mu$ g of protein was deposited on a quartz window and dried under a stream of Argon. The films were then rehydrated via the vapor phase and sealed using a second window. Raman spectra were obtained on a Bruker Senterra confocal Raman microscope using 785 nm laser excitation at room temperature. A laser power of 100 mW was used with 300 s of integration time. The Raman scattered light was dispersed onto a CCD (Andor, iDus, South Windsor CT) at a 3–5  $\text{cm}^{-1}$  resolution. A background of buffer and  $\text{CaF}_2$  was subtracted from each spectrum measured.

Samples were left for 24 h in a darkened room to test for evidence of dark adaptation. A 300 s dark spectrum was acquired, followed by illumination with the halogen lamp for >5 min. A second 300 s spectrum was acquired immediately afterward and subtracted.

## 3. Results

### GPR and BPR Have Very Similar Chromophore Structures

Figure 1 compares GPR WT and BPR WT spectra at pH 9.5. The resonance Raman spectrum (532 nm excitation)<sup>28</sup> and FT Raman spectrum (1064 nm excitation)<sup>8</sup> have previously been reported only for GPR and at lower resolution. The GPR spectrum in Figure 1 agrees with the earlier reported spectra, although as expected the intensity of some bands are different due to the dependence of Raman intensity on exciting wavelength. The most intense band is the ethylenic stretch vibration at 1536  $\text{cm}^{-1}$  in GPR and 1552  $\text{cm}^{-1}$  in BPR. The upshift of 16  $\text{cm}^{-1}$  of the major ethylenic mode is expected on the basis of an empirical linear correlation between the visible absorption wavelengths and the ethylenic stretch frequency observed for other rhodopsins.<sup>29</sup>

Bands between 1150 and 1300  $\text{cm}^{-1}$  which include C–C single bond stretching modes of the retinal are sensitive to the isomeric configurations of the retinal chromophore.<sup>30</sup> The BPR spectrum has bands at 1162, 1172, 1185, and 1200  $\text{cm}^{-1}$  which correspond almost exactly in frequency and intensity to bands in GPR at 1162, 1172, 1185, and 1198  $\text{cm}^{-1}$  indicating that the retinal conformation of the two species is almost identical. Earlier studies have identified these bands as characteristic of the all-*trans* configuration of retinal.<sup>30,31</sup> For example, in bacteriorhodopsin, bands appear in the all-*trans* state in this region at 1169, 1184, and 1201  $\text{cm}^{-1}$ .<sup>30</sup> In BR, a partial switch occurs thermally to a 13-*cis* configuration in the dark which

is evident by changes in the fingerprint region and also the appearance of bands at 800 and 1348  $\text{cm}^{-1}$ .<sup>30</sup> However in the case of GPR and BPR, no evidence was found of dark adaptation after leaving the sample in the dark for 24 h.

Bands from 1000–800  $\text{cm}^{-1}$  include the hydrogen-out-of-plane (HOOP) modes of the chromophore which are also sensitive to chromophore conformation. HOOP modes are expected to have little intensity for planar polyenes,<sup>29,32</sup> but twists around single and double bonds which create a nonplanar configurations produce intensification of these modes in the RRS.<sup>32-34</sup> In contrast to previous studies<sup>8,28</sup> which only noted a band at 959  $\text{cm}^{-1}$ , several bands were observed in this region which are candidates for HOOP modes based on their similarity with the BR spectrum.<sup>30</sup> The largest peaks in this region appear at 959, 899, 878, and 822  $\text{cm}^{-1}$  in both GPR and BPR with similar intensity indicating that the out-of-plane structure of retinal polyene due to torsions around single and double bounds is very similar in the unphotolyzed states of GPR and BPR, as well as BR (959, 898, 882, and 830  $\text{cm}^{-1}$ ).<sup>30</sup>

### Environment of the Schiff base in GPR and BPR is different

A band near 1640  $\text{cm}^{-1}$  in the RRS of BR was assigned to the  $\text{C}=\text{N}$  stretching vibration of the protonated Schiff base (SB).<sup>15</sup> In the case of GPR purified on a phenylsepharose column and solubilized in octylglucoside (OG), a doublet at 1643 and 1656  $\text{cm}^{-1}$  was previously reported<sup>28</sup> and attributed to the presence of two different forms of GPR. In the current study where GPR is reconstituted in *E. coli* polar lipids (see Materials and Methods), only a single band is observed at 1654  $\text{cm}^{-1}$ . A single band at a similar, but not identical frequency (1657  $\text{cm}^{-1}$ ) is found in BPR (see Figure 2). The difference of 3  $\text{cm}^{-1}$  was highly reproducible based on more than 4 independently prepared samples of GPR and BPR.

In order to confirm that these bands are due to the  $\text{C}=\text{N}$  SB vibration, GPR and BPR were regenerated using a  $\text{C}15\text{-}^2\text{H}$  labeled retinal (see Materials and Methods), which is expected to produce a downshift in the  $\text{C}=\text{N}$  stretch frequency. For example in BR this causes a downshift from 1640 to 1629  $\text{cm}^{-1}$ <sup>31</sup> and in HR from 1633 to 1627  $\text{cm}^{-1}$ .<sup>35</sup> As seen in Figure 2, the band in GPR undergoes a similar  $\text{C}15\text{-}^2\text{H}$  induced shift of 11  $\text{cm}^{-1}$  whereas BPR undergoes a smaller shift of 6  $\text{cm}^{-1}$ . There is also an indication that a shoulder still remains in the isotope labeled samples near 1655  $\text{cm}^{-1}$  likely due to a small contribution from the amide I vibration of the protein backbone. This is not unexpected due to the preresonance 785 nm excitation and the fact that the amide I mode of the protein should be relatively intense relative to other protein vibrations.

Hydrogen/deuterium (H/D) exchange was used to probe the hydrogen bonding strength of the SB in GPR and BPR. H/D exchange induces a downshift in  $\text{C}=\text{N}$  frequency which has previously been related to the strength of the SB-counterion hydrogen-bond.<sup>15,36</sup> The differences in GPR (23  $\text{cm}^{-1}$ ) and BPR (21  $\text{cm}^{-1}$ ) are significantly larger than in BR (16  $\text{cm}^{-1}$ ) indicating a stronger hydrogen bond strength in both proteorhodopsins. However, even after repeated exposure of the sample to  $\text{D}_2\text{O}$  a small band remains near 1656  $\text{cm}^{-1}$ , again indicating the presence of a contribution at this frequency from the amide I vibration. The differences in both the frequency of the  $\text{C}=\text{N}$  stretching vibration and the H/D induced downshift while small were highly reproducible. Furthermore, as discussed below the differences depend on the identity of the residue 105, thus indicating that this residue largely controls the differences in environment of the retinal Schiff base in GPR and BPR.

### Difference Detected in Interaction of Residue 105 with the Retinylidene C13-Methyl Group in BPR and GPR

In addition to the ethylenic stretch frequency between GPR and BPR, the most striking difference occurs in the methyl rock region of the spectrum (1000–1020  $\text{cm}^{-1}$ ). This band in

principle could be assigned to either methyl group in the retinylidene chromophore (C13, C9), however based on the evidence presented below, it is most likely assigned predominantly to the C13 methyl rock vibration. GPR has a single band similar in frequency to BR at  $1006\text{ cm}^{-1}$  (Figure 3) in agreement with earlier studies.<sup>8,28,37</sup> BPR has a more intense peak which is shifted to  $1012\text{ cm}^{-1}$  with a shoulder near  $1004\text{ cm}^{-1}$  (Figure 4). This frequency is higher compared to the many other microbial rhodopsins studied including BR, SRI, SRII, and HR.<sup>17,21,23,24</sup> In the case of BR, the band frequency has been found to shift when Leu93, the homologous residue for Leu105 in GPR, is substituted with an Ala.<sup>38</sup> This is not surprising since Leu93 is located close to the C13-methyl group in BR as determined by high resolution crystallographic structures.<sup>39</sup> This residue has also been shown to influence the 13-*cis* to all-*trans* isomerization in the late N to O transition of the photocycle of BR.<sup>38</sup>

In order to determine if residue 105 in GPR and BPR also interact with the C13-methyl group in retinal the RRS of several mutants were measured. The GPR L105Q and L105E mutants shift the methyl rock band to  $1010\text{ cm}^{-1}$ , very similar to BPR (Figure 3). The reciprocal mutation in BPR (Q105L) shows the ethylenic C=C stretch and the SB C=N stretch frequencies of GPR and BPR are switched in the mutants GPR L105Q and BPR Q105L, respectively (Figure 4). For example, the bands at  $1655$ ,  $1538$ , and  $1006\text{ cm}^{-1}$  in BPR Q105L match almost exactly the bands in GPR WT. Note that in the GPR L105Q mutant the ethylenic band at  $1542\text{ cm}^{-1}$  is not fully restored to the frequency in BPR in agreement with the partial shift of the visible maximum from  $523$  to  $498\text{ nm}$  (not the full blue-shifted value observed in BPR of  $488\text{ nm}$ ).<sup>13</sup>

A mutant replacing leucine 105 with a polar asparagine exhibits a methyl rock band at  $1007\text{ cm}^{-1}$ , very close to the GPR WT frequency of  $1006\text{ cm}^{-1}$ . This residue is smaller than glutamine by a single carbon, yet it has almost no effect on color tuning (see inset to Figure 3). This shows C13 methyl interaction with values resembling GPR WT. This shows that the distance of residue 105 to the retinal is of crucial importance in determining the interaction with the SB and C13 methyl group. In agreement, when a glutamic acid residue replaces Gln 105, the methyl stretch bands appear at  $1009$  and  $1004\text{ cm}^{-1}$ , close to WT BPR. Due to the similarity in frequency, the carboxyl group is most likely neutral, even at pH 9.5. The side chain is the same length as a glutamine and therefore in a position to interact with both the SB and the C13 methyl group.

To test the hypothesis that the residue at position 105 is substantially responsible for the differences in the hydrogen bonding strength of the Schiff base in GPR and BPR, H/D exchange was measured for the mutant BPR Q105L. This caused a downshift of the  $1655\text{ cm}^{-1}$  band by  $23\text{ cm}^{-1}$  to  $1632\text{ cm}^{-1}$  (Figure 5), exactly the same as the H/D induced downshift of the Schiff base in GPR WT. The L105Q mutant of GPR showed a reduced shift of  $20\text{ cm}^{-1}$  from  $1655$  to  $1635\text{ cm}^{-1}$  similar to the H/D induced downshift in BPR WT (Figure 6).

### Substitution of the BPR Sequence in GPR after Helices A–C Does Not Affect Its Chromophore Vibrational Spectrum

In order to test whether residues other than at position 105 account for the observed differences in the RRS of GPR and BPR, chimeras of GPR and BPR were expressed and measured. One chimera designated G3B4 consisted of the first three helices of GPR and the final four helices of BPR (see Materials and Methods). A second chimera designated B3G4 consisted of the first three helices and BPR and the last four helices of GPR. The G3B4 spectrum shown in Figure 4 has a leucine at residue 105 and is almost identical to the GPR WT spectrum particularly in the methyl rock, ethylenic and Schiff base vibrations. The H/D induced shift of the Schiff base frequency is exactly the same as in GPR WT and BPR

Q105L mutant (Figure 5). This result demonstrates that none of the sequence differences in helices D–G between GPR and BPR have an influence on the overall chromophore structure in the unexcited state. This result provides further evidence that the differences observed are attributable to residue 105 and its inferred interaction with the C13 methyl group and Schiff base. In the case of B3G4, the spectrum resembles BPR including an upshift of the methyl-rock mode to  $1010\text{ cm}^{-1}$ . However the ethylenic stretch vibration at  $1545\text{ cm}^{-1}$  is not at the same value as BPR indicating that other residues in helices D–G may also play a role in the chromophore environment. In agreement the wavelength of the visible absorption at 496 nm does not fully shift to that of BPR at 488 nm.<sup>13</sup> One possibility is that residue Glu 142 on helix D which has recently been determined to exist in a protonated state in GPR but ionized state in BPR, may play a role in this difference.<sup>40</sup>

## 4. Discussion

This study compares the resonance Raman spectra of the two most extensively studied representatives of the GPR and BPR classes of proteorhodopsins. These two variants are typical of the two major classes in general and have visible absorption maxima near 532 and 488 nm, respectively. The visible wavelength maxima are believed to have evolved to match the spectral environment of the different marine photic zones which these variants occupy.<sup>2–12</sup> Although both GPR and BPR are capable of pumping protons using solar energy,<sup>2</sup> BPR is exposed to a much lower photon flux at 75 m depth compared to the more shallow waters where GPR exists. At least for the GPR and BPR variants thus far characterized BPR exhibits a much slower photocycle compared to GPR (200 ms vs 20 ms).<sup>10</sup> This difference has led to the suggestion that the primary function of BPR may not be the utilization of solar energy to power cellular processes as in the case for GPR<sup>10,41</sup> but rather a photoregulatory function. Although the visible absorption properties of BPR and GPR have been modeled using the high resolution structures of BR and SRII,<sup>41,42</sup> a high resolution crystallographic structure for any PR has not yet been elucidated. Hence, an atomic structural basis for the different properties of BPR and GPR is currently unknown.

A key observation is that switching residue 105 in GPR (Leu) to BPR (Gln) reverses the visible absorption maximum and photocycle time back to the BPR phenotype.<sup>10,13</sup> One proposed model suggests that spectral tuning may derive from the altered hydrogen bonding of the chromophore charge complex when polar side groups are nearby.<sup>13</sup> The homologous residue in mouse cone rhodopsins causes a similar effect.<sup>43</sup> The RRS data of the residue 105 mutants confirms that the hydrophobicity and length of the side chain will directly change the environment of the SB.

It is noted that the RRS measurements were performed at pH 9.5. The generally accepted typical value for the pH of seawater is 8.3. The  $pK_a$  of the Schiff base proton acceptor in proteorhodopsins (Asp 97) is approximately 7.5,<sup>10,40</sup> and an ionized acceptor Asp is required for their proton transport activity. The presence of the nonfunctional acid form (e.g., which is substantial at pH 8.3) complicates molecular spectroscopic analysis by creating a subpopulation of molecules with an altered nonproductive photocycle with different photointer-mediate.<sup>44–46</sup> Therefore, to have a homogeneous population of functional pumping forms of BPR, it is necessary to make measurements at pH well above the Asp  $pK_a$ . Studies of proteorhodopsins are generally made at alkaline pH values; we choose 2 pH units above the Asp  $pK_a$  to ensure that >99% of the molecules are functionally active in proton transport. This pH is consistent with many other published papers on proteorhodopsin including studies using resonance Raman spectroscopy (pH 9.5),<sup>28</sup> FTIR (pH 9.5),<sup>47</sup> (pH 9.2–10)<sup>8</sup> and (pH 8.5),<sup>9</sup> ultrafast visible and IR (pH 9.5)<sup>48,49</sup> and NMR and EM (pH 10).<sup>50</sup>

Our measurements reveal that the chromophore conformation of GPR and BPR are very similar. For example, differences in the retinal structure in the polyene chain would be expected to result in significant changes in frequencies and intensities of the C–C stretching and HOOP modes of the chromophore are not observed. On the other hand, the observed changes in the ethylenic stretching frequency between BPR and GPR can occur without a significant change in chromophore structure such as predicted by the point charge model of retinal chromophore color tuning.<sup>51</sup> In this model, polar and charged groups near the SB cause alterations in the bond conjugation along the polyene chain thereby leading to changes in the absorption wavelengths.

Despite the strong similarity of the GPR and BPR RRS, one major difference which cannot be accounted for as a direct consequence of alteration in the polyene bond conjugation is the shift in the methyl-rock frequency from 1006 cm<sup>-1</sup> in GPR to 1012 cm<sup>-1</sup> in BPR. In particular, normal mode calculations reflect only pure methyl rock vibrations in this region.<sup>30,52</sup> Instead, the changes observed most likely reflect real differences in the interaction of this C13-methyl group with the residue at position 105. In particular, our evidence shows that the methyl-rock shift is almost completely reversible depending on the presence of a leucine or glutamine residue in position 105. The wavelength of visible absorption (and correlated ethylenic stretch) is also sensitive to other substitutions. However, replacement of an asparagine for a leucine cause nearly no shift as compared to the GPR WT even though asparagine is nearly as hydrophilic as glutamine.

A second finding is the detection of a shift in the hydrogen bonding strength of the Schiff base depending on the identity of residue 105. Although the difference of the H/D induced downshift is relatively small (~2–3 cm<sup>-1</sup>) it is consistently reproduced in not only GPR/BPR but mutants of GPR or BPR that switch the visible absorption, e.g. a small H/D induced shift is associated with the BPR blue-shifted visible absorption. This pattern is also preserved in the chimeras G3B4 and B3G4 as discussed above and hence appears to be highly correlated with the change in visible absorption and ethylenic stretch frequency.

A model that accounts for all of these findings is shown in Figure 7. BPR and GPR are modeled using a high resolution structure of BR<sup>39</sup> with the homologous residue Leu93 in BR replaced by Gln or Leu, respectively. In the case of BPR (see Figure 7, right panel), the Gln105 C $\gamma$ –C $\delta$  bond has been rotated so that the NH group of the Gln residue interacts directly with the Schiff base with a distance of 3.97 Å while the oxygen atom on the Gln105 carbonyl group is 2.91 Å away from the carbon of the C13 methyl. This model fits the RRS data indicating an interaction of Gln105 with both the methyl group and the SB. In the case of GPR, a water molecule is hypothesized to be present near Leu105 which interacts directly with the Schiff base (see Figure 7, left panel) instead of Gln105. Further evidence for the existence of this model is found from low-temperature FTIR difference measurements on BPR.<sup>53</sup>

Note that in this model, a hydrogen bond is formed with the Schiff base either from the Gln residue (BPR) or from a water molecule in the case of GPR. Hence the environment near the Schiff base is expected to be similar but not exactly the same as deduced by RRS. In addition the interaction with the C13-methyl retinal group is expected to be considerably different since in one case a nonpolar Leu residue is located nearby whereas in the case of BPR the polar C=O group of Gln is present.

## 5. Conclusions

We have compared the resonance Raman spectra of two forms of proteorhodopsin and found that despite their different absorption and photochemical characteristics, their RR spectra are

remarkably close. The spectral similarity shows that the retinal chromophore is in a nearly identical environment in both proteins. However, two differences between GPR and BPR are evident, namely the environments of the C13 methyl group and of the Schiff base. These differences can be explained by a molecular model involving the replacement of Leu105 (GPR) with Gln105 (BPR). This simple substitution has profound effects on spectral tuning and photocycle rate and is possibly related to different functions in the native organisms.

## Acknowledgments

We thank Dr. Weiwu Wang for his assistance with plasmid constructions and Dr. Jason Amsden for his helpful comments. This work was supported by National Institutes of Health Grants R01GM069969 (to K.J.R.) and R37GM27750 (to J.L.S.), Department of Energy Grant DE-FG02-07ER15867, and the Robert A. Welch foundation (to J.L.S.).

## References and Notes

- (1). Beja O, Aravind L, Koonin EV, Suzuki MT, Hadd A, Nguyen LP, Jovanovich SB, Gates CM, Feldman RA, Spudich JL, Spudich EN, DeLong EF. *Science*. 2000; 289:1902. [PubMed: 10988064]
- (2). Beja O, Spudich EN, Spudich JL, Leclerc M, DeLong EF. *Nature*. 2001; 411:786. [PubMed: 11459054]
- (3). de la Torre JR, Christianson LM, Beja O, Suzuki MT, Karl DM, Heidelberg J, DeLong EF. *Proc. Natl. Acad. Sci. U.S.A.* 2003; 100:12830. [PubMed: 14566056]
- (4). Venter JC, Remington K, Heidelberg JF, Halpern AL, Rusch D, Eisen JA, Wu D, Paulsen I, Nelson KE, Nelson W, Fouts DE, Levy S, Knap AH, Lomas MW, Nealson K, White O, Peterson J, Hoffman J, Parsons R, Baden-Tillson H, Pfannkoch C, Rogers YH, Smith HO. *Science*. 2004; 304:66. [PubMed: 15001713]
- (5). Rusch DB, Halpern AL, Sutton G, Heidelberg KB, Williamson S, Yooseph S, Wu D, Eisen JA, Hoffman JM, Remington K, Beeson K, Tran B, Smith H, Baden-Tillson H, Stewart C, Thorpe J, Freeman J, Andrews-Pfannkoch C, Venter JE, Li K, Kravitz S, Heidelberg JF, Utterback T, Rogers YH, Falcon LI, Souza V, Bonilla-Rosso G, Eguiarte LE, Karl DM, Sathyendranath S, Platt T, Bermingham E, Gallardo V, Tamayo-Castillo G, Ferrari MR, Strausberg RL, Nealson K, Friedman R, Frazier M, Venter JC. *PLoS Biol.* 2007; 5:e77. [PubMed: 17355176]
- (6). Spudich JL. *Trends Microbiol.* 2006; 14:480. [PubMed: 17005405]
- (7). Sabehi G, Beja O, Suzuki MT, Preston CM, DeLong EF. *Environ. Microbiol.* 2004; 6:903. [PubMed: 15305915]
- (8). Dioumaev AK, Brown LS, Shih J, Spudich EN, Spudich JL, Lanyi JK. *Biochemistry*. 2002; 41:5348. [PubMed: 11969395]
- (9). Friedrich T, Geibel S, Kalmbach R, Chizhov I, Ataka K, Heberle J, Engelhard M, Bamberg E. *J. Mol. Biol.* 2002; 321:821. [PubMed: 12206764]
- (10). Wang WW, Sineshchekov OA, Spudich EN, Spudich JL. *J. Biol. Chem.* 2003; 278:33985. [PubMed: 12821661]
- (11). Gomez-Consarnau L, Gonzalez JM, Coll-Llado M, Gourdon P, Pascher T, Neutze R, Pedros-Alio C, Pinhassi J. *Nature*. 2007; 445:210. [PubMed: 17215843]
- (12). Bielawski JP, Dunn KA, Sabehi G, Beja O. *Proc. Natl. Acad. Sci. U.S.A.* 2004; 101:14824. [PubMed: 15466697]
- (13). Man D, Wang W, Sabehi G, Aravind L, Post AF, Massana R, Spudich EN, Spudich JL, Beja O. *Embo J.* 2003; 22:1725. [PubMed: 12682005]
- (14). Mathies R, Freedman TB, Stryer L. *J. Mol. Biol.* 1977; 109:367. [PubMed: 839546]
- (15). Lewis A, Spoonhower J, Bogomolni RA, Lozier RH, Stoerkenius W. *Proc. Natl. Acad. Sci. U. S. A.* 1974; 71:4462. [PubMed: 4530995]
- (16). Mendelsohn R, Verma AL, Bernstein HJ, Kates M. *Can. J. Biochem.* 1974; 52(9):774. [PubMed: 4425972]
- (17). Campion A, El-Sayed MA, Terner J. *Biophys. J.* 1977; 20(3):369. [PubMed: 922125]



- (18). Argade PVR, Kenneth J. *Biochemistry*. 1983; 22:3460.
- (19). Argade PV, Rothschild KJ, Kawamoto AH, Herzfeld J, Herlihy WC. *Proc. Natl. Acad. Sci. U.S.A.* 1981; 78:1643. [PubMed: 6785758]
- (20). Smith SO, Lugtenburg J, Mathies RA. *J. Membr. Biol.* 1985; 85:95. [PubMed: 4009698]
- (21). Fodor SP, Gebhard R, Lugtenburg J, Bogomolni RA, Mathies RA. *J. Biol. Chem.* 1989; 264:18280. [PubMed: 2808377]
- (22). Dratz EA, Furstenau JE, Lambert CG, Thireault DL, Rarick H, Schepers T, Pakhlevanians S, Hamm HE. *Nature*. 1993; 363:276. [PubMed: 8487866]
- (23). Gellini C, Luttenberg B, Sydor J, Engelhard M, Hildebrandt P. *FEBS Lett.* 2000; 472:263. [PubMed: 10788623]
- (24). Alshuth T, Stockburger M, Hegemann P, Oesterhelt D. *FEBS Lett.* 1985; 179(1)
- (25). Bergo VB, Ntefidou M, Trivedi VD, Amsden JJ, Kralj JM, Rothschild KJ, Spudich JL. *J. Biol. Chem.* 2006; 281:15208. [PubMed: 16537532]
- (26). Shi L, Yoon SR, Bezerra AG Jr, Jung KH, Brown LS. *J. Mol. Biol.* 2006; 358:686. [PubMed: 16530786]
- (27). Rath P, Krebs MP, He Y-W, Khorana HG, Rothschild KJ. *Biochemistry*. 1993; 32:2272. [PubMed: 8443170]
- (28). Krebs RA, Dunmire D, Partha R, Braiman MS. *J. Phys. Chem. B.* 2003; 107:7877.
- (29). Aton B, Doukas AG, Callender RH, Becher B, Ebrey TG. *Biochemistry*. 1977; 16:2995. [PubMed: 880292]
- (30). Smith SO, Braiman MS, Myers AB, Pardo JA, Courtin JML, Winkel C, Lugtenburg J, Mathies RA. *J. Am. Chem. Soc.* 1987; 109:3108.
- (31). Smith SO, Myers AB, Mathies RA, Pardo JA, Winkel C, Van den Berg EMM, Lugtenburg J. *Biophys. J.* 1985; 47(5)
- (32). Eyring G, Curry B, Mathies R, Fransen R, Palings I, Lugtenburg J. *Biochemistry*. 1980; 19:2410. [PubMed: 7387982]
- (33). Braiman M, Mathies R. *Proc. Natl. Acad. Sci. U.S.A.* 1982; 79:403. [PubMed: 6281770]
- (34). Rothschild KJ, Marrero H, Braiman M, Mathies R. *Photochem. Photobiol.* 1984; 40:675. [PubMed: 6514815]
- (35). Smith SO, Marvin MJ, Bogomolni RA, Mathies RA. *J. Biol. Chem.* 1984; 259:12326. [PubMed: 6490613]
- (36). Baasov T, Friedman N, Sheves M. *Biochemistry*. 1987; 26:3210. [PubMed: 3607019]
- (37). Bergo V, Amsden JJ, Spudich EN, Spudich JL, Rothschild KJ. *Biochemistry*. 2004; 43:9075. [PubMed: 15248764]
- (38). Subramaniam S, Greenhalgh DA, Rath P, Rothschild KJ, Khorana HG. *Proc. Natl. Acad. Sci. U.S.A.* 1991; 88:6873. [PubMed: 1650486]
- (39). Luecke H, Schobert B, Richter HT, Cartailler JP, Lanyi JK. *J. Mol. Biol.* 1999; 291:899. [PubMed: 10452895]
- (40). Kralj JM, Bergo VB, Amsden JJ, Spudich EN, Spudich JL, Rothschild KJ. *Biochemistry*. 2008; 47:3447. [PubMed: 18284210]
- (41). Hillebrecht JR, Galan J, Rangarajan R, Ramos L, McCleary K, Ward DE, Stuart JA, Birge RR. *Biochemistry*. 2006; 45:1579. [PubMed: 16460005]
- (42). Rangarajan R, Galan JF, Whited G, Birge RR. *Biochemistry*. 2007; 46:12679. [PubMed: 17927209]
- (43). Sun H, Macke JP, Nathans J. *Proc. Natl. Acad. Sci. U.S.A.* 1997; 94:8860. [PubMed: 9238068]
- (44). Huber R, Kohler T, Lenz MO, Bamberg E, Kalmbach R, Engelhard M, Wachtveitl J. *Biochemistry*. 2005; 44:1800. [PubMed: 15697205]
- (45). Imasheva ES, Balashov SP, Wang JM, Dioumaev AK, Lanyi JK. *Biochemistry*. 2004; 43:1648. [PubMed: 14769042]
- (46). Lakatos M, Lanyi JK, Szakacs J, Varo G. *Biophys. J.* 2003; 84:3252. [PubMed: 12719254]
- (47). Krebs RA, Alexiev U, Partha R, DeVita AM, Braiman MS. *BMC Physiol.* 2002; 2:5. [PubMed: 11943070]

- (48). Rupenyan A, van Stokkum IH, Arents JC, van Grondelle R, Hellingwerf K, Groot ML. *Biophys. J.* 2008; 94:4020. [PubMed: 18234812]
- (49). Amsden JJ, Kralj JM, Chieffo LR, Wang X, Erramilli S, Spudich EN, Spudich JL, Ziegler LD, Rothschild KJ. *J. Phys. Chem. B.* 2007; 111:11824. [PubMed: 17880126]
- (50). Shastri S, Vonck J, Pflieger N, Haase W, Kuehlbrandt W, Glaubitz C. *Biochim. Biophys. Acta.* 2007; 1768:3012. [PubMed: 17964280]
- (51). Honig B, Dinur U, Nakanishi K, Balogh-Nair V, Gawinowicz MA, Arnaboldi M, Motto MG. *J. Am. Chem. Soc.* 1979; 101:7084.
- (52). Smith SO, Pardo JA, Lugtenburg J, Mathies RA. *J. Phys. Chem.* 1987; 91:804.
- (53). Amsden JJ, Kralj JM, Bergo VB, Spudich EN, Spudich JL, Ziegler LD, Rothschild KJ. *J. Phys. Chem. B.* 2007; 111:11824. [PubMed: 17880126]

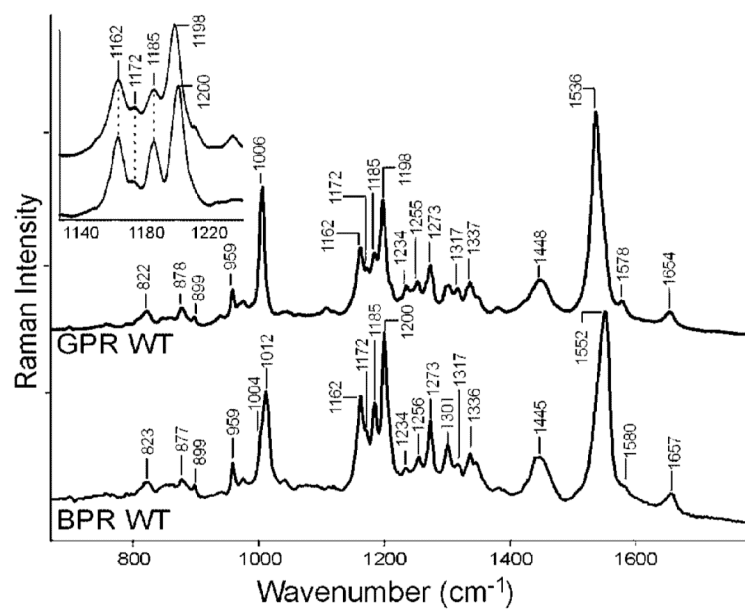


**Figure 1.** RRS of the green (GPR) and blue (BPR) blue absorbing proteorhodopsins. Data was taken using a 785 nm probe laser for 300 s. A background spectrum of the quartz coverslip and buffer was subtracted from the sample data. The spectra were scaled using the intensity of the ethylenic peak at 1536/1552  $\text{cm}^{-1}$ .

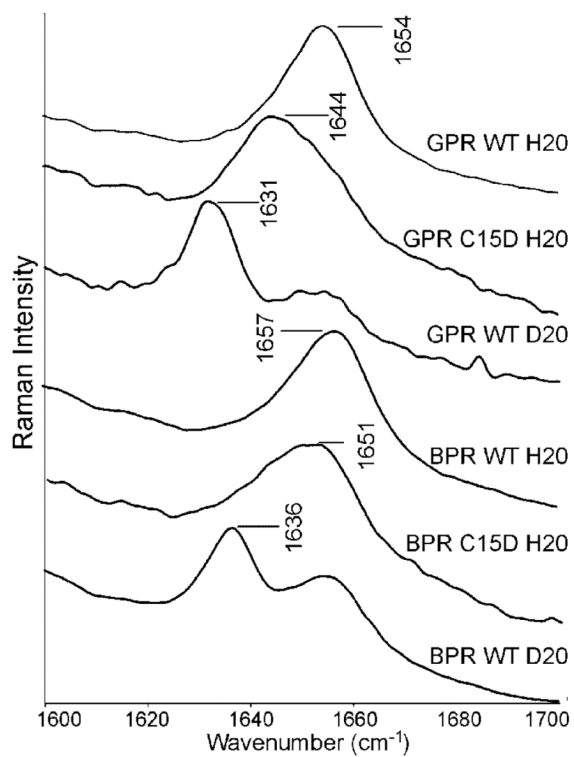


**Figure 2.** The RRS of the region showing the C=N stretch of the Schiff base. The assignment is made on the basis of C15D and D<sub>2</sub> O exchange.

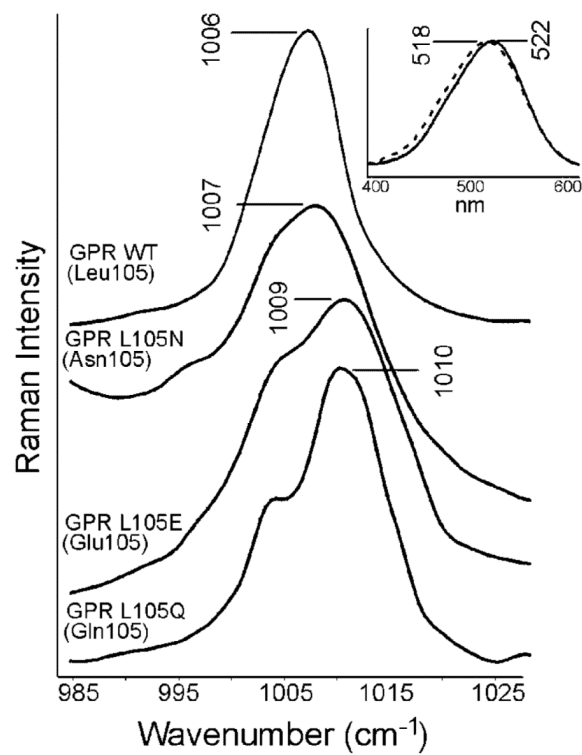


**Figure 3.** The resonance Raman spectra of GPR WT and mutants in the methyl rock region. Inset shows the visible absorption of GPR WT (solid) and GPR L105N (dashed). Even with a polar asparagine at residue 105, it still shows the GPR WT phenotype.

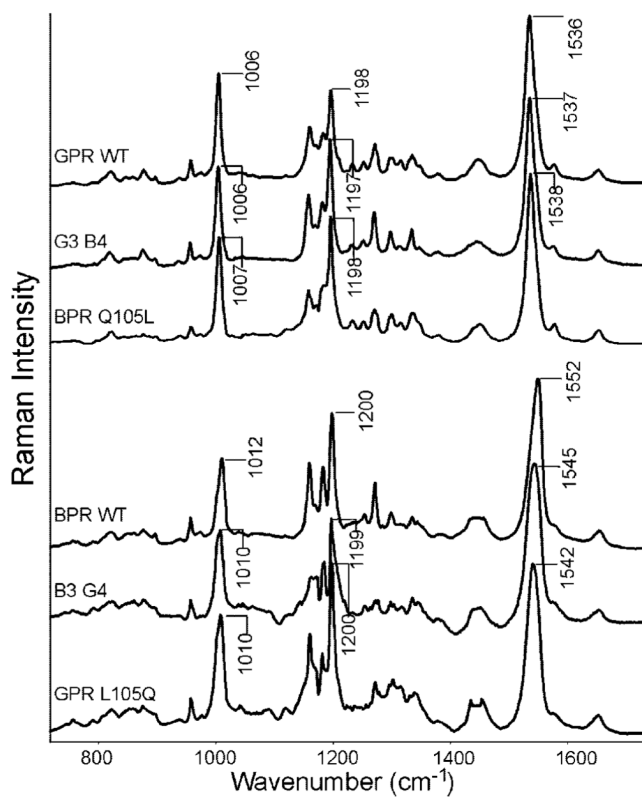


**Figure 4.** Top three plots: RRS spectra of proteorhodopsins with leucine at position 105, GPR WT, G3B4 chimera, and BPR Q105L. Bottom three plots: RRS spectra of proteorhodopsins with glutamine at residue 105; BPR WT, B3G4 chimera, GPR Q105L. All data were scaled to the ethylenic peaks.

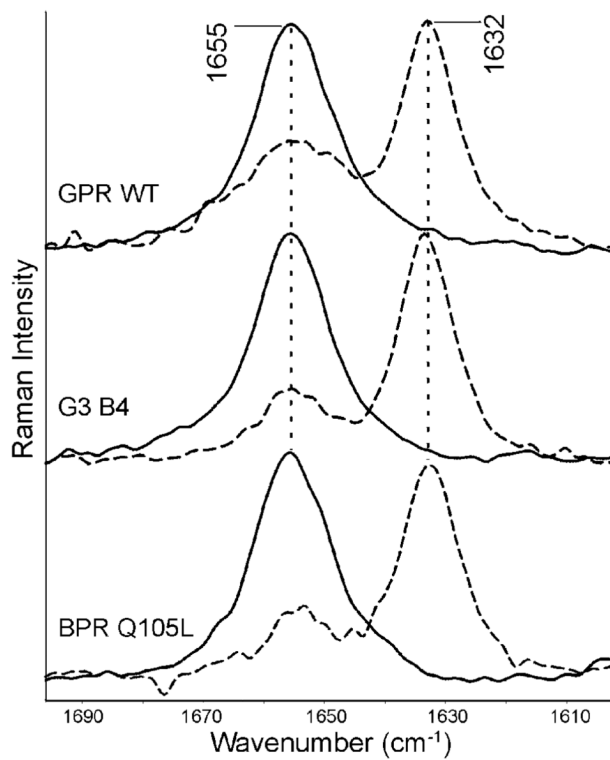


**Figure 5.** Resonance Raman spectra of the  $C=N$  vibration of the Schiff base for the GPR WT, G3B4 chimera, and BPR Q105L mutant all with a leucine at residue 105. The  $H_2O$  spectrum (solid) is compared to the  $D_2O$  spectrum (dashed) to reveal the H-bond strength of the counterion.

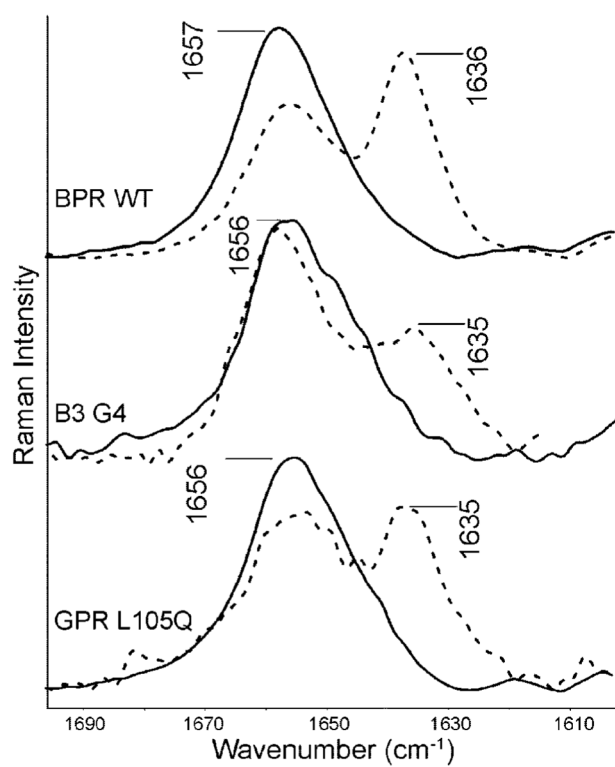


**Figure 6.** Resonance Raman spectra of the C=N vibration of the Schiff base for the BPR WT, B3G4 chimera, and GPR L105Q mutant all with a glutamine at residue 105. The H<sub>2</sub>O spectrum (solid) is compared to the D<sub>2</sub>O spectrum (dashed).



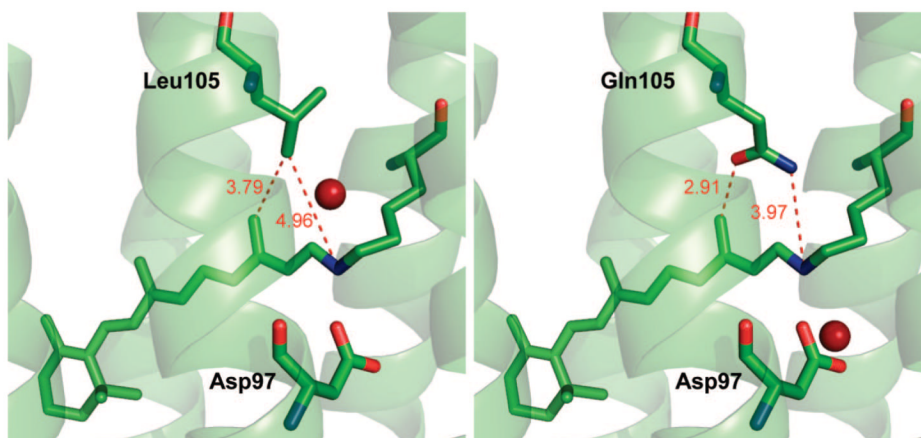


**Figure 7.** Models of GPR (left) and BPR (right) based on the BR structure (pdb file 1C3W<sup>39</sup>). The replacement of leucine with glutamine in the case of BPR shows that Gln105 is in a position to interact both with the Schiff base as well as the C13 methyl group. In the case of GPR, a water molecule has been inserted which is located 2.91 Å away from the Schiff base nitrogen. Distances shown in Å.